

Boundary-Layer Transition on a Body of Revolution

G.C. Lauchle,* J.J. Eisenhuth,† and G.B. Gurney‡

Applied Research Laboratory, The Pennsylvania State University, State College, Pa.

The laminar-to-turbulent transition region was measured over a body length Reynolds number range of 9.55-47.7 million on a large, streamlined, axisymmetric body sting mounted in the Applied Research Laboratory's 1.22 m diameter water tunnel. Theoretical calculations of the transition Reynolds numbers for this body shape were carried out and the results were correlated with the experimental data. It is shown that good correlation can be achieved if e^n is chosen as the transition criterion in the linear stability calculations, where n is an empirical number, which depends on the freestream turbulence intensity. It was found that this number approached 9 for those test velocities where the freestream turbulence intensity is on the order of 0.1%.

Introduction

BOUNDARY-layer transition on axisymmetric bodies is of practical importance because its location influences the total skin frictional drag of the body. It is well recognized that moving the transition point downstream to larger body arc length positions results in drag reduction. Consequently, much of the current research is dealing with boundary-layer control concepts such as temperature differentials at the wall and surface suction.

The Applied Research Laboratory at The Pennsylvania State University is actively engaged in transition research from both the analytical and experimental points of view. Experiments are generally designed for the 1.22 m diameter water tunnel located at this laboratory. This facility is particularly suited for such work because of the high water velocities that can be attained (up to 19.8 m/s), the ability to test large bodies (~0.50 m in diameter and ~3.5 m long), and the fact that settling section turbulence management results in test section turbulence intensities that are quite low (~0.1 %). Under normal operating water temperatures (25°C) this water tunnel has an upper unit Reynolds number of approximately 21 million/m.

By way of preliminary preparation for planned experiments on bodies with various types of boundary-layer control, the work described in this paper was carried out. After a candidate body shape was selected and a test model fabricated, experiments were performed in the 1.22 m diameter water tunnel to acquire baseline transition data and in-tunnel body pressure distributions. Except for the hydrodynamic shape of this body, no boundary-layer control was employed in these experiments. The results of the pressure distribution measurements are presented elsewhere.¹

In addition to the experimental results, theoretical calculations for the growth of linear disturbances in the laminar boundary layer are also described for the test body. These calculations were performed using the methods of Gentry and Wazzan,² where the body pressure distribution (which is a required input) was calculated from potential flow theory and corrected for inviscid tunnel interference effects.^{3,4} The transition location may be deduced from this

type of calculation by choosing some amplification, which is usually expressed in terms of e^n . The value of n is difficult to predict for most flows because it is influenced by so many factors. These factors include the effects of freestream disturbances such as turbulence, particulates, and noise as well as surface effects such as roughness, waviness, vibration, temperature, and normal fluid velocity (suction or blowing).

In the current experimental investigation we have minimized the surface and environmental effects as much as possible. Body roughness and waviness were held to less than 0.8 μm (rms) and 127 μm in 0.1 m of length, respectively. Of course, no suction, blowing, or wall temperature differentials were used. The particulates in the water tunnel are usually smaller than 25 μm because this is the size filter used during routine filling, draining, and bypass operations. Measurements have shown that the standard deviation of the particulate distribution is 2.1 μm and that they number about 10⁶/liter (5.2×10^{-8} % of the water volume). Because the body was tested without any auxiliary machinery such as propellers and drivetrains, the background noise and vibration levels were relatively low, although quantitative data were not acquired. Thus, the major factor to influence e^n is freestream turbulence. In presenting the experimental results and in the correlation of these data with the theoretical results, an attempt will be made to deduce the appropriate values of n as a function of the freestream turbulence intensity.

Test Body and Experimental Techniques

The body selected for experimental studies in transition and transition control is described mathematically by:

$$\hat{y} = \sqrt{\hat{x}(2 - \hat{x})} - K_n \frac{C_0 \hat{x}}{2a^2} \exp\left\{-\frac{\hat{x}^2}{2a^2} - kK_n\right\} + \hat{x}^2 \epsilon_L \quad (1)$$

where x and r are the axial and radial coordinates of the body and where $\hat{x} = x/\ell_n$, ℓ_n = nose length, $\hat{y} = r/D_{\max}/2$, D_{\max} = maximum diameter of the body, $K_n = \ell_n/D_{\max}$, and a , C_0 , and k are numerical constants. The parameter

$$\epsilon_L = \frac{K_n C_0}{2a^2} \exp\left\{-\frac{1}{2a^2} - kK_n\right\} \quad (2)$$

The tailcone is formed by an 18 deg arc of radius

$$R_L = \frac{2.5 D_{\max}}{2 \sin(18 \text{ deg})} \quad (3)$$

An inflection curve is then faired between the end of the arc (at $\phi = 90 - 18 = 72$ deg) and a 4 in. diam disk whose center is

Received April 11, 1980; revision received Aug. 20, 1980. Copyright © American Institute of Aeronautics and Astronautics, Inc., All rights reserved.

Index categories: Boundary-Layer Stability and Transition; Computational Methods; Hydrodynamics.

*Senior Research Associate, Applied Research Laboratory.

†Associate Professor of Aerospace Engineering, Department of Aerospace Engineering and Applied Research Laboratory. Member AIAA.

‡Assistant Professor of Engineering Research, Applied Research Laboratory.

coincident with the axis of symmetry. In the current program, $a=0.3$, $C_0=0.0303$, $k=0.45227$, $\ell_n=2.438$ m, $D_{\max}=0.324$ m, and L , which is the total body length (nose plus tailcone), is 3.05 m. This body was fabricated from fiberglass and is sting mounted in the water tunnel. As noted previously, the surface finish was held to within given tolerances. However, there are discrete areas where these tolerances have not been met, which are at the locations of the pressure taps (a total of 94 throughout the total length) installed during the initial fabrication. These taps were required so that the in-tunnel body pressure distributions could be measured. In order to minimize the effect that these taps may have on transition, all measurements were performed on the opposite side of the body from the taps. Figure 1 shows the shape of the test body as calculated from Eq. (1) and with it the theoretical and experimental pressure distributions. The potential flow calculation^{3,4} includes the inviscid tunnel blockage effects, and the corrected curve includes the viscous effects.¹

Transition detection may be performed by a variety of techniques. The simplest method involves a measurement of the total pressure close to the body surface with a small, "hypodermic needle size" pitot probe. The probe is traversed downstream until a sudden increase in pressure is observed which results from the thickening of the boundary layer at transition. This method is not practical for water-tunnel measurements (especially at high speeds) because of the mechanical strength required in a traversing apparatus. Furthermore, the technique does not allow detailed acquisition of the fluctuating components of velocity or pressure which are important to know from the viewpoints of linear stability theory and other spectral descriptions of the transition process.

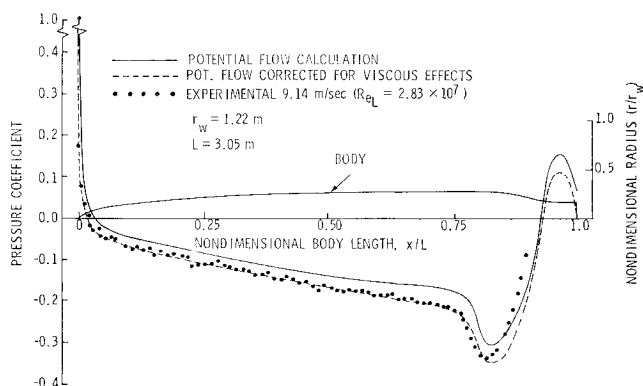


Fig. 1 Body shape and its in-tunnel body pressure distributions (data from Ref. 1).

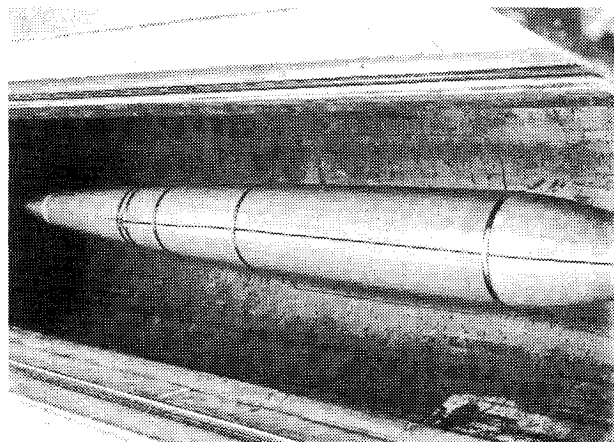


Fig. 2 View of test body sting mounted in 1.22 m diam water tunnel; also shown is hot-film probe secured to body.

Dynamic sensors are, therefore, most useful in detailed measurements of the transition zone. In the laminar part of the flow, the signal from a dynamic velocity or pressure sensor is essentially smooth. Farther downstream where disturbances begin to amplify, the signal may be somewhat periodic (wavelike). Eventually these waves (Tollmein-Schlichting waves) become very unstable and nonlinear; bursts of turbulence appear and the signal is intermittent. The flow remains intermittent for a region that depends on many factors: Reynolds number, pressure gradient, and disturbance level to note a few. Eventually the signal becomes totally random indicating that the boundary layer is fully turbulent. Under some conditions, the boundary layer will change abruptly from laminar to turbulent with no measurable trace of periodic or intermittent flow regimes. This form of transition is commonly referred to as "bypass" transition.

In this experimental investigation, two dynamic transition probes were used. One was pressure sensitive while the other was velocity sensitive (hot-film probe). The pressure-sensitive probe was simply a strain-gaged pressure transducer mounted in a streamlined, pencil-shaped housing. The housing provided a resonant chamber and acoustic waveguide so that the effective active area of the transducer was reduced to a pinhole size.

The hot-film probe used in these experiments was a standard parabolic probe manufactured by Thermo-Systems. The mounting scheme was the same for this probe as it was for the pressure-sensitive probe. A streamlined probe holder was fabricated that blended smoothly with the body contour and supported the probe at a slight angle relative to the tangent line of the body at the point of mounting. This holder, as well as the lead wire, was held to the body with adjustable stainless steel bands. Figure 2 shows the body in the tunnel and a typical arrangement for holding the transition probes. The sensitive elements of the probes were nominally 0.25 mm from the surface of the body.

The procedure used in these experiments was to secure the probe at a given point on the body corresponding to a known value of arc length s . The tunnel was then filled with fresh water and the flow velocity slowly increased until the speed corresponding to each of the various flow regimes (laminar, wavelike, intermittent, and fully turbulent) was identified by observing the probe signal displayed on an oscilloscope. It was found that the pressure probe could clearly delineate between laminar and fully turbulent flow, but the cavity resonance (2 kHz) made it difficult to identify the wavelike or intermittent flow regimes.

In presenting the experimental transition data, a transition Reynolds number defined by

$$Re_t = u_e s / \nu \quad (4)$$

will be used. Here, u_e is the boundary-layer edge velocity at transition, i.e.,

$$u_e = U_{\infty} \sqrt{1 - C_p(s)} \quad (5)$$

where $C_p(s)$ is the potential flow pressure coefficient at that value of arc length s where the probe was located and U_{∞} is the tunnel speed at which fully turbulent flow occurred at the probe. The tunnel velocity was measured with a pitot-static probe located 0.75 m upstream of the body nose plane and 0.1 m from the tunnel wall. The water temperature remained at 21°C throughout these experiments; therefore, the kinematic viscosity $\nu = 1.007 \times 10^{-6}$ m²/s. The freestream velocity ranged over 3.05-15.24 m/s which corresponds to a unit Reynolds number range of 3.03 - 15.13×10^6 /m.

The turbulence intensity in the test section has been measured over a range of flow conditions and is reported by Robbins.⁵ He extended those measurements to lower velocities and the results to be published later are shown in Fig. 3. Considerable scatter in the data exists for flow

velocities less than 7.5 m/s. It is speculated that this scatter is due to nonsteady flow within the honeycomb located in the settling section. That is, at these lower velocities, the Reynolds number of the honeycomb cells is believed to be near a critical value; hence, some cells may sustain laminar flow while others are turbulent. Because of momentum deficits, these flow states would move from cell to cell in a random manner and perhaps cause the turbulence fluctuations in the test section to become nonstationary.

Theoretical

The method used to predict transition makes use of linear stability theory. The computational code used in this type of calculation is the Transition Analysis Program System (TAPS).² Amplification rates for disturbances at discrete frequencies result from this calculation. The frequencies are determined from the real part of the complex eigenvalues of a modified Orr-Sommerfeld equation. The amplification rates are the imaginary parts of these eigenvalues. The pressure distribution used for input into this and subsequent boundary-layer computations is given by the solid line curve of Fig. 1.

Figure 4 shows a typical result from this type of calculation for a freestream velocity of $U_\infty = 15.21$ m/s and 21°C water temperature. The natural logarithm of $a/a_0 = A$ is expressed as a function of body arc length for discrete nondimensional circular frequencies, $\omega\nu/U_\infty^2$. The ratio A represents the increase in magnitude of a boundary-layer disturbance with respect to an initial disturbance amplitude a_0 . The point at which $A=1$ ($=e^0$) defines the neutral stability point. A transition point may be obtained from this representation by forming an envelope around the family of curves (one curve for each frequency) and choosing a suitable amplification, a choice not easily made. Based on the many transition experiments performed on bodies, plates, and airfoils, this amplification has been found to vary from as low as e^5 to as high as e^{14} . A commonly used value which seems to fit much of the data is e^9 . However, it is also known that the exponent ($\ln A$) is a function of ambient disturbances such as freestream turbulence, noise, surface finish, or vibration. A quantitative dependence of $\ln A$ at transition on the various disturbances has yet to be established.

Mack⁶ has attempted to resolve the dependence of transition on freestream turbulence. An empirical formula which he developed is

$$n = -8.43 - 2.4 \ln(u'/U_\infty) \quad (6)$$

where u'/U_∞ is the streamwise component of turbulence intensity. The number n is the suggested exponent to use in

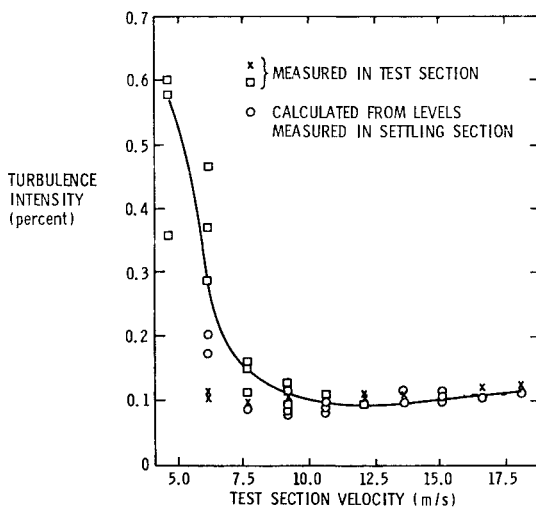


Fig. 3 Freestream turbulence intensity levels in test section of 1.22 m diam water tunnel.

identifying the transition point from linear stability curves when freestream turbulence is known to exist. It is noted that the above relation is based solely on flat-plate data. Mack has subsequently proceeded to devise a more general theory that should have wider application. It uses actual disturbance amplitudes made up of all harmonic components and orientations. This more general theory has not been applied in the present investigation because only a limited number of the special functions arising from the analysis have been evaluated.⁶

To explain the experimental data obtained in this investigation, two transition criteria will be used with curves such as the ones shown in Fig. 4, e^9 and e^n . The values for n are calculated from Eq. (6) using the turbulence intensities identified by the solid line of Fig. 3. In addition to comparing the e^9 and the e^n transition point predictions, neutral stability points are compared, one calculated from TAPS (e^0 point) and the other by a method due to Schlichting.⁷ The pressure gradient parameter $\Lambda = (\delta^2/\nu)(du_e/ds)$ required for the Schlichting method was calculated using an axisymmetric, implicit finite-difference solution of the boundary-layer equations of motion. Here, δ is the laminar boundary-layer thickness.

Results

As noted previously, the transition point is defined as that point on the body where the flow becomes fully turbulent with no intermittency, and the transition Reynolds number is a function of freestream velocity. From Fig. 3, u'/U_∞ changes with U_∞ ; consequently a transition Reynolds number measured at a given value of U_∞ must also be interpreted in terms of a given value of freestream turbulence intensity. The dependence of the measured transition Reynolds number on freestream turbulence is thus shown in Fig. 5. Note that those data points located at 0.1% turbulence level were measured at the highest test velocity (15.24 m/s) which corresponds to a unit Reynolds number of $15.13 \times 10^6/\text{m}$. Also shown on this figure are flat-plate transition data measured by Wells⁸ and Schubauer and Skramstad.⁹ The current data follow the same trends with turbulence intensity as do those for the flat-plate flows. It appears that the transition Reynolds number asymptotically approaches 4×10^6 as the turbulence intensity approaches zero. It is of interest to note that Re_t does not fall off quite as rapidly as the Wells data as u'/U_∞ increases above 0.1%. This behavior may be due to the stabilizing effect of the favorable pressure gradient that occurs on the axisymmetric body. The various flow regimes observed using the hot-film transition probe are indicated in Fig. 6. These experimental data have been compared with predicted spatial amplification ratios of disturbances as calculated by linear stability theory.² The e^9 criterion predicts transition velocities

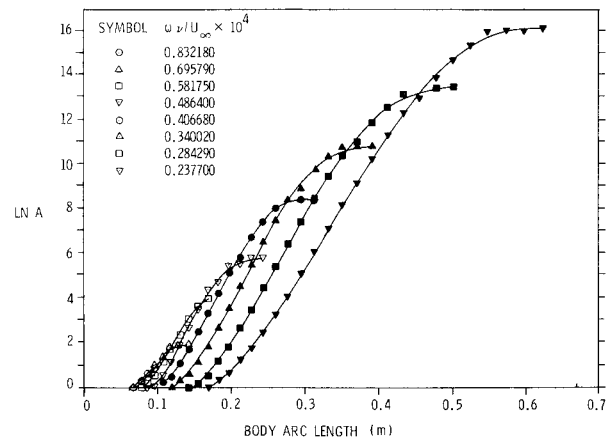


Fig. 4 Linear stability calculations for test body at $Re_L = 4.62 \times 10^7$ and $Re_U = 1.51 \times 10^7/\text{m}$.

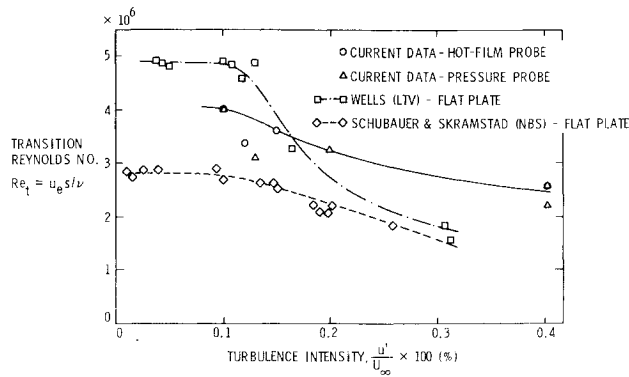


Fig. 5 Transition Reynolds numbers for test body expressed in terms of freestream turbulence levels.

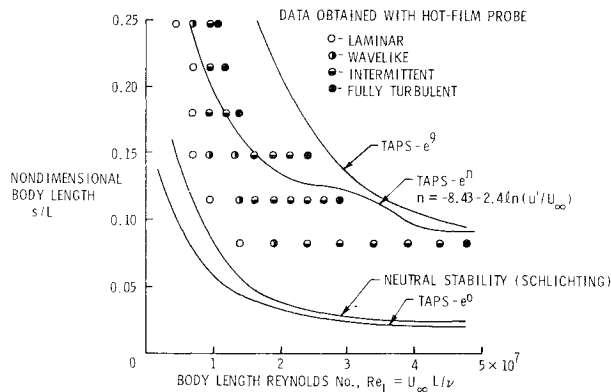


Fig. 6 Various flow regimes observed experimentally on test body.

that are higher than those observed experimentally for a given position of the probe. On the other hand, the e^n criterion [n calculated from Eq. (6) using u' / U_∞ from Fig. 3] results in predictions that compare quite favorably with the data. It is seen that the e^9 and e^n curves tend to converge to the experimental data as the body length (or unit) Reynolds number becomes large. This is due to the fact that $n \rightarrow 9$ as Re_L increases, i.e., the turbulence intensity is on the order of 0.1% at these Reynolds numbers and $n = 8.2$. Also shown in Fig. 6 are the predicted neutral stability curves for this body. They fall well within the laminar flow regime of the body as would be expected. At the higher Reynolds numbers ($Re_L > 2 \times 10^7$), the TAPS and Schlichting results agree very well.

The experimentally determined transition arc lengths at various body length Reynolds numbers are shown in Fig. 7. Of course, these represent the same data as presented in Fig. 6, but the ordinate has been expanded so that some transition data acquired by Northrop Corp. in the late 1950s¹⁰ could be included for comparative purposes. These Northrop transition data were obtained on an elliptically shaped body very similar to the one used here. Its length was 2.44 m and the data were obtained by in-flight experimental methods. In comparing the two sets of data, excellent agreement is seen. The Northrop body does maintain laminar flow to slightly longer arc lengths, but this may possibly be due to the differences in surface finish and freestream turbulence. Again, the theoretical e^n criterion predicts transition points that are in very good agreement with those observed experimentally.

Transition Reynolds numbers are expressed in terms of body length Reynolds number in Fig. 8. The current data agree quite well with the Northrop data as well as with the TAPS e^n predictions. The e^9 predictions agree well only at body length Reynolds numbers greater than about 3×10^7 which corresponds to turbulence levels of 0.1%.

It is seen that Re_t increases with Re_L for both bodies. Presumably, the Northrop data, being acquired during flight

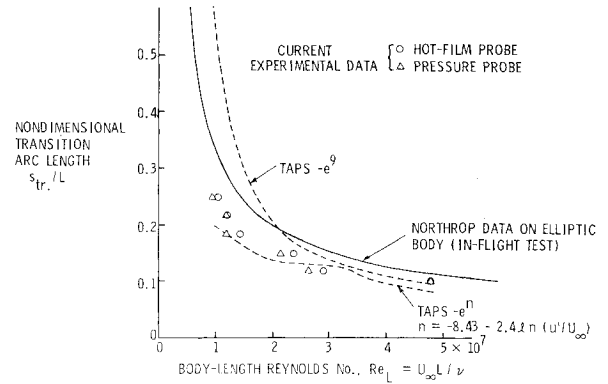


Fig. 7 Transition arc lengths measured on and predicted for test body as function of body length Reynolds number.

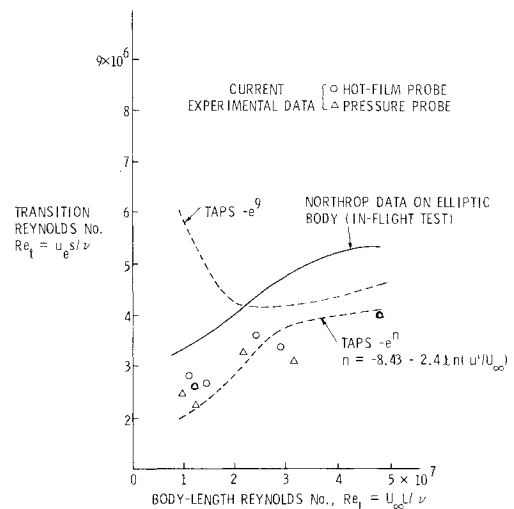


Fig. 8 Measured and predicted transition Reynolds numbers for test body as function of body length Reynolds number.

tests, is unaffected by freestream turbulence disturbances. On the other hand, the water-tunnel data do appear to be affected by freestream turbulence at the lower test velocities. This has been deduced from the agreement between the data and the e^n prediction, where n varied between 3.84 and 8.2. One should therefore not expect the two sets of experimental data to compare as favorably as they do. Without any detailed description of the atmospheric disturbance level or of the vibro/acoustic disturbance level encountered during the Northrop tests, this anomaly is difficult to resolve.

Conclusions

In this experimental investigation, the laminar-to-turbulent transition region has been measured on a large streamlined body of revolution operating in a 1.22 m diameter water tunnel. Theoretical predictions of the transition points were performed using linear stability theory. Neutral stability points were predicted using the linear stability theory as well as an approximate approach due to Schlichting. The theoretical and experimental transition points and transition Reynolds numbers were compared over a range of body length Reynolds numbers. Under these experimental conditions, the freestream turbulence intensity has been characterized, thus enabling the transition data to be expressed in terms of freestream turbulence intensity.

Based on the results of the experiments and of the theoretical predictions, several conclusions may be made:

1) Under all experimental conditions, transition from laminar to turbulent flow took place in a natural manner, going through wavelike and intermittent regimes before

becoming fully turbulent. No bypass transition was observed.

2) The experimental data follow specific trends with body length Reynolds number; the same trends that were observed during in-flight transition measurements on a Northrop elliptic body operating over the same Reynolds number range.

3) Because it is known that the freestream turbulence intensity in the water tunnel increases at lower velocities ($U_\infty < 9.14$ m/s), the transition amplification ratio of the linear stability calculations was adjusted to account for this effect. The exponent of e was selected according to an empirical formula developed by Mack.⁶ This exponent n is a function of the freestream turbulence intensity and was found to vary from 3.84 at a freestream velocity of 3.05 m/s to 8.2 for velocities greater than 9.12 m/s. The correlation between the e^n linear stability transition point prediction and the experimentally observed transition locations was found to be very good.

4) It was found for those values of Reynolds number ($Re_L > 3 \times 10^7$ or $Re_U = U_\infty/\nu > 9.84 \times 10^6/\text{m}$) where the freestream turbulence intensity is on the order of or less than 0.1%, that the measured transition locations agree quite well with both the e^9 and the e^n ($n = 8.2$) linear stability predictions. The fact that an e^9 transition point agrees so well with one using the $e^{8.2}$ criterion may be explained in terms of the rate at which a disturbance grows on this body. It may be seen from Fig. 4 that $d(\ln A)/ds$ is on the order of 13/m, which means that a change in exponent of 0.8 results in a change of only 61 mm in transition location.

With regard to future work, a second body of the same shape and size as the one described in this paper is currently being fabricated. However, it will have an electric heat exchanger so that the surface may be heated above the ambient temperature of the water. With a heated surface, many of the laminar boundary-layer disturbances should be damped through a mechanism of viscosity variation within the laminar layer. It is anticipated that the transition Reynolds numbers will be increased significantly above those presented in this paper. Body drag will also be measured in this future program and its dependence on surface temperature, transition Reynolds number, etc., established. Eisenhuth and Hoffman¹¹ have developed a methodology for predicting the wall temperature required to maximize the transition Reynolds number of a given body under given flow conditions. This technique has been applied in the design of the heat exchanger for this new body.

Acknowledgment

This work has been supported by the U.S. Naval Sea Systems Command, Code 63R-31. The authors are grateful for this support.

References

- ¹Lauchle, G.C., "Horizontal Buoyancy Effects on the Pressure Distribution of a Body in a Duct," *Journal of Hydronautics*, Vol. 13, April 1979, pp. 61-67.
- ²Gentry, A.E., and Wazzan, A.R., "The Transition Analysis Program System Vol. II-Program Formulation and Listings," McDonnell Douglas Corp., Report MDC J7255-02, June 1976.
- ³Hess, J.L. and Martin R.P., Jr., "Improved Solution for Potential Flow about Arbitrary Axisymmetric Bodies by the Use of a Higher Order Surface Source Method; Part I, Theory and Results," NASA CR 134694, MDC J6627-01, July 1974.
- ⁴Friedman, D.M., "Improved Solution for Potential Flow About Arbitrary Axisymmetric Bodies by the Use of a Higher-Order Surface Source Method: Part II. User's Manual for Computer Program," NASA CR 134695, MDC J6627-02, July 1974.
- ⁵Robbins, B.E., "Water Tunnel Turbulence Measurements Behind a Honeycomb," *Journal of Hydronautics*, Vol. 12, July 1978, pp. 122-128.
- ⁶Mack, L.M., "On the Effects of Free-Stream Turbulence on Boundary-Layer Transition," Paper presented at the 2nd RAND Transition Workshop, Santa Monica, Calif., Sept. 13-15, 1976.
- ⁷Schlichting, H., *Boundary Layer Theory*, 6th Ed., McGraw-Hill Book Co., N.Y., 1968.
- ⁸Wells, C.S., Jr., "Effects of Free-Stream Turbulence on Boundary-Layer Transition," *AIAA Journal*, Vol. 5, Jan. 1967, pp. 172-174.
- ⁹Schubauer, G.B. and Skramstad, H.K., "Laminar Boundary-Layer Oscillations and Transition on a Flat Plate," NACA Report 909, 1948.
- ¹⁰Groth, E.E., "Boundary Layer Transition on Bodies of Revolution," Northrop Aircraft, Report NAI-57-1162, July 1957 (unpublished).
- ¹¹Eisenhuth, J.J. and Hoffman, G.H., "A Simplified Method for Predicting Body Temperature Distribution in the Preliminary Design of Heated Underwater Bodies," TM 79-02, Applied Research Laboratory, The Pennsylvania State University, June 4, 1979.